



OPEN

Controlling nitrogen migration through micro-nano networks

SUBJECT AREAS:

AGRI-ECOLOGY
POLLUTION REMEDIATION
ORGANIC-INORGANIC
NANOSTRUCTURES
STRUCTURAL PROPERTIESDongqing Cai^{1,2}, Zhengyan Wu^{1,2}, Jiang Jiang^{1,2}, Yuejin Wu^{1,2}, Huiyun Feng^{1,2}, Ian G. Brown³, Paul K. Chu⁴ & Zengliang Yu^{1,2}

¹Key Laboratory of Ion Beam Bioengineering of Chinese Academy of Sciences & Anhui Province, Hefei 230031, People's Republic of China, ²Bioenergy Forest Research Centre of State Forestry Administration, Hefei 230031, People's Republic of China, ³Lawrence Berkeley National Laboratory, Berkeley CA 94720, USA, ⁴Department of Physics and Materials Science, City University of Hong Kong, Hong Kong, People's Republic of China.

Received
6 June 2013Accepted
2 December 2013Published
14 January 2014Correspondence and
requests for materials
should be addressed to
Z.L.Y. (zlyu@ipp.ac.
cn)

Nitrogen fertilizer unabsorbed by crops eventually discharges into the environment through runoff, leaching and volatilization, resulting in three-dimensional (3D) pollution spanning from underground into space. Here we describe an approach for controlling nitrogen loss, developed using loss control fertilizer (LCF) prepared by adding modified natural nanoclay (attapulgite) to traditional fertilizer. In the aqueous phase, LCF self-assembles to form 3D micro/nano networks via hydrogen bonds and other weak interactions, obtaining a higher nitrogen spatial scale so that it is retained by a soil filtering layer. Thus nitrogen loss is reduced and sufficient nutrition for crops is supplied, while the pollution risk of the fertilizer is substantially lowered. As such, self-fabrication of nano-material was used to manipulate the nitrogen spatial scale, which provides a novel and promising approach for the research and control of the migration of other micro-scaled pollutants in environmental medium.

With the widespread use of fertilizers and high-temperature industrial combustion, mankind has doubled the rate at which nitrogen is removed from the atmosphere relative to pre-industrial times, contributing to acid rain, eutrophication and worsening global warming^{1–4}. The Intergovernmental Panel on Climate Change (IPCC) has reported that approximately 1.25% of nitrogen fertilizer used is emitted in the form of N₂O. The concentration of atmospheric N₂O has increased 16% over the last 250 years at a rate of 0.25% per year. N₂O is approximately 300 times more potent in absorbing thermal radiation compared with carbon dioxide (CO₂) and also has a long residence time in the atmosphere (120 years)⁵. Also, atmospheric N₂O plays an important role in the acidification of land and water ecosystems through dry and wet deposition such as acid rain^{6,7}. In China, active nitrogen (NO₂) pollution in the gas caused by nitrogen fertilizer has also been widely concerned⁸. Furthermore, lost fertilizer nutrition directly contributes to soil acidification. China is now the world's largest producer and consumer of synthetic nitrogen fertilizers. Overuse of N fertilizer contributes substantially to regional soil acidification in China. Soil pH declined significantly from the 1980s to the 2000s in major Chinese crop-production areas³. Nitrogen fertilizers also cause water eutrophication. It has been reported by Gregory that a 2.5-fold increase of nitrate concentration occurred in the Mississippi River during the period 1960–1998. This nitrate flux could have been reduced by 33% if the use of nitrogen-containing fertilizer in the Mississippi River basin had been cut by 12%¹. In China, the annual nitrogen input to Lake Taihu has been estimated at 4,282 tons, more than a half of which is from cropland. This accumulation of nitrogen has been directly linked to frequent algal blooms in recent years⁹.

During the past 20 years, various types of controlled/slow release fertilizer have been developed using coatings, urine enzyme inhibitors, nitrification inhibitors, urea formaldehyde, etc^{10–13}. Although these products effectively enhance N use efficiency, the released unabsorbed N tends to be transferred into the environment through runoff, leaching and volatilization. In the future, chemical agriculture may be replaced by organic agriculture, however, the decomposed organic N has the same migration problem before being absorbed by crops. Thus we believe that controlling nitrogen migration is a fundamental and promising countermeasure to reduce the environmental risk of fertilization. In this article, we report on the development of a novel N-migration controlling approach using a new kind of fertilizer, called loss control fertilizer (LCF). When added with the appropriate amount of modified attapulgite, N fertilizer can self-assemble into three-dimensional (3D) micro/nano networks through hydrogen bonds and molecular forces so as to increase the N spatial scale which actually refers to the spatial scale of the N fertilizer networks. Therefore the N migration and loss can be controlled via the filtering effect of soil. The



resulting reduction of N loss and increase of available nutrition are beneficial for both crop yield and environment protection. Since 2006, LCF has been widely applied (more than 3.4 million hectares) in China, presenting outstanding agricultural (yield increases more than 10%) and environmental effects (N loss decreases more than 20%) compared with traditional fertilizer with equal nutrition. Herein, loss control urea (LCU) or loss control NH_4Cl (LCN) was used as the model LCFs to investigate the detailed microstructure, interactions in LCF and loss control performance.

Results

LCU is a ternary system composed of attapulgite, polyacrylamide (P) and urea (U). Attapulgite ($\text{Si}_8\text{O}_{20}\text{Mg}_5(\text{Al})(\text{OH})_2(\text{H}_2\text{O})_4 \cdot 4\text{H}_2\text{O}$) is a kind of natural rod-like inorganic nano material with rod diameter of 20–50 nm and length of $1 \mu\text{m}^{14}$. Naturally, attapulgite rods tend to aggregate to form bunches (Fig. 1a), which is the dominant disadvantage in practice. In this work, attapulgite was treated by O_3 oxidation and hydrothermal process in order to improve the dispersion (Fig. 1b) and the $-\text{OH}$ number on the surface, which might facilitate the formation of micro-nano networks and combination with urea molecules. Such dispersed attapulgite was named ATP and mixed with P (2%, W/W) to obtain a loss control agent (LCA) which was thereafter added to urea or NH_4Cl (W/W, LCA/fertilizer = 1/9) to obtain LCU or LCN.

U-P and U-ATP can form specific morphologies under various aqueous conditions (Supplementary Fig. 1). U-P can self fabricate to form scolopendra-like interpenetrating networks (actually fractal

structure) in aqueous solution. After being mixed with U, ATP was found to own higher dispersion, which was probably due to the hydrogen bonds between U and ATP. Interestingly, U-ATP-P (actually LCU) showed a directional micro/nano network surface in aqueous solution (Fig. 1c). After washing repeatedly with distilled water, a 3D complex directional network skeleton within LCU exposed and could be clearly seen (Fig. 1d). From the TEM image in Fig. 1e, a similar network skeleton composed of nano-rods with high density was also observed within LCU. Moreover, the rods were proved to be mainly ATP by element mapping analysis. The network skeleton (Fig. 1e) consisted mainly of Al, Si and Mg and the superposition image (Fig. 1f) of their distribution maps coincided well with the skeleton. These results illustrate that ATP within LCU has formed 3D networks, and U or P contributes significantly to ATP's dispersion and the formation of the 3D directional network skeleton.

As seen in the hard X-ray images (Fig. 2a–c) and video (Supplementary video 1) by synchrotron radiation, ATP alone exists as numerous independent aggregates (pH 7.0) other than networks, while its dispersion is improved with increasing pH due to the increase of the zeta potential (absolute value) of ATP (Supplementary Fig. 2). That is to say, ATP alone is unable to form a network structure. Nevertheless, the ATP within LCU displayed a high dispersion and few aggregates could be found. More importantly, these ATP rods transform into 3D networks through connection with each other, shown in the X-ray images (Fig. 2d–f) and video (Supplementary video 2). This result is also consistent with the morphology shown in Fig. 1. Besides, the ATP networks and the Mg distribution

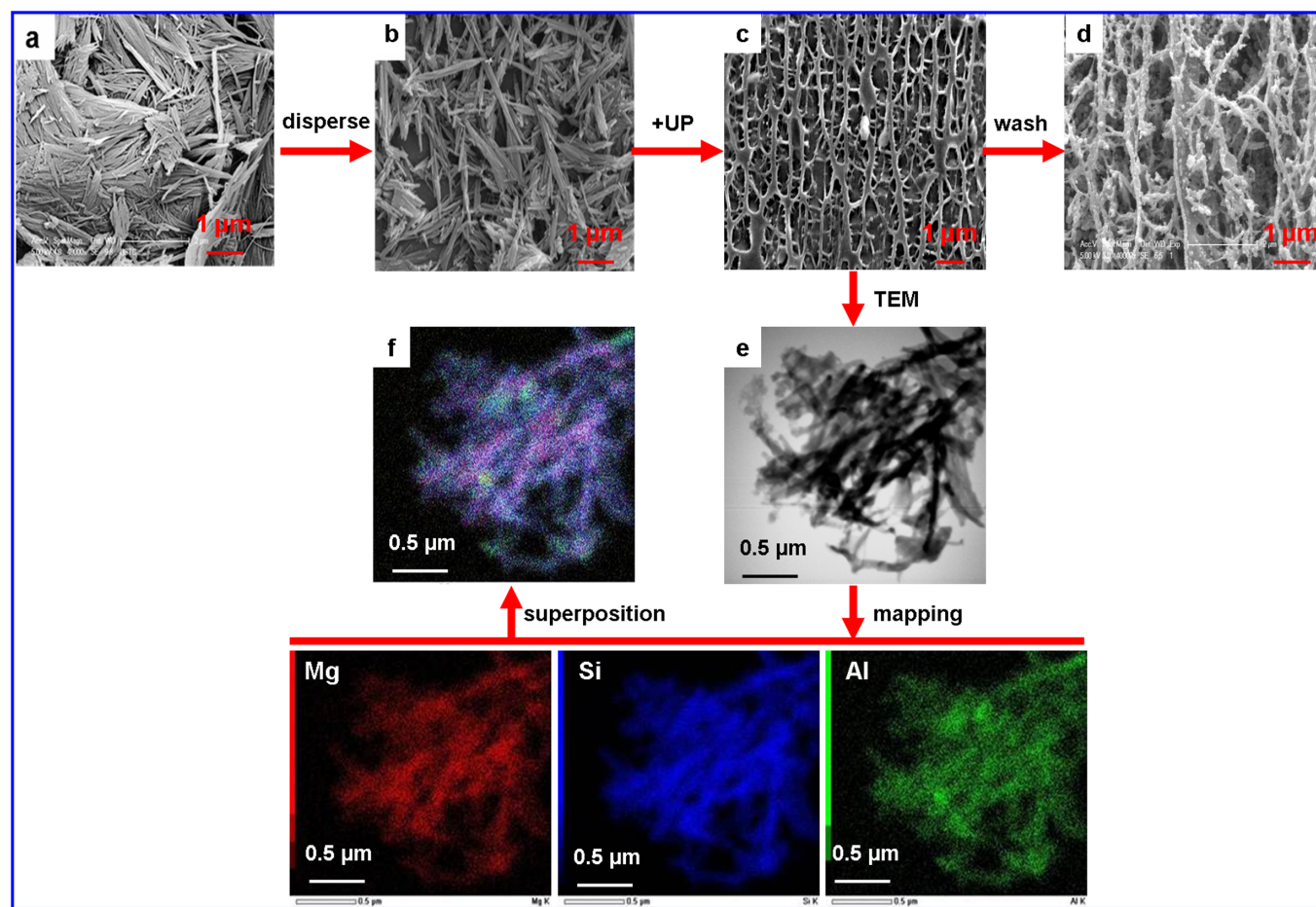


Figure 1 | Morphology of LCU system. (a–d), Scanning electron microscopy (SEM) images of “bunch” structure of natural attapulgite, ATP, directional micro/nano network surface of LCU in aqueous solution (3 g/L, pH 7, 30°C) and 3D complex directional network skeleton within water-washed LCU respectively. (e), Transmission electron microscope (TEM) image of the network skeleton composed of ATP nano rods within LCU. (f), Superposition image of three distribution maps (Al, Si and Mg) in the skeleton.

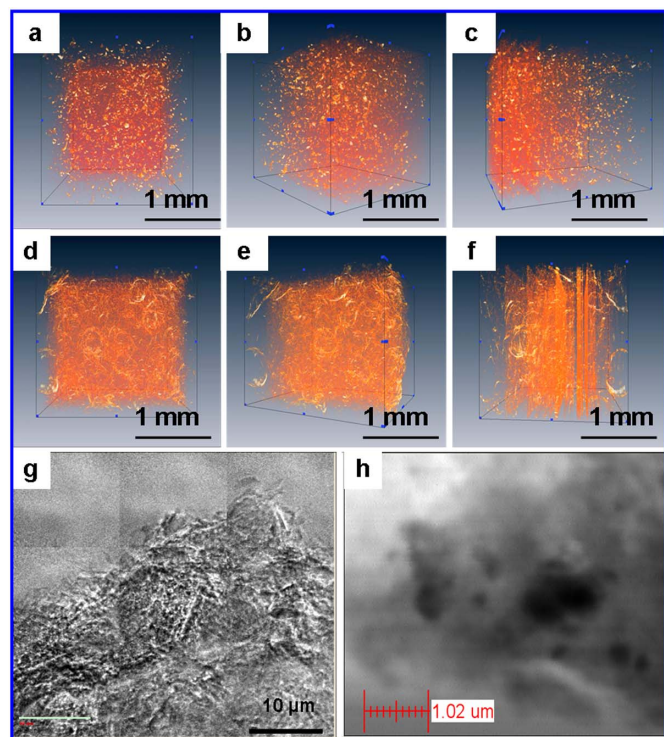


Figure 2 | Microstructure of LCU by synchrotron radiation X-ray imaging system. (a–c), Aggregate structure and distribution of natural attapulgite from three different angles by synchrotron radiation hard X-ray imaging system (SRHX). (d–f), 3D micro/nano network structure and distribution of ATP within LCU from three different angles by SRHX. (g,h), Micro/nano network structure of ATP (g) and Mg distribution (h) within LCU by scanning and transmission X-ray (soft) microscopy (STXM) on synchrotron radiation (1314 eV). The brighter regions in (g) correspond to ATP rods, and the organics (mainly urea and few P) are embedded within the ATP meshes.

can also be achieved by scanning and transmission X-ray microscopy (STXM) on synchrotron radiation, wherein the brighter regions imply ATP rods (Fig. 2g), which is further verified by the Mg distribution (Fig. 2h). In addition, the matter embedded within the ATP meshes should be organics (mainly urea and a few P) (Fig. 2g).

To simulate practical application conditions (irrigation, rain and so on), the LCU sample was buried within the top layer of a sand column followed by leaching with distilled water (Supplementary Fig. 3). LCU tends to self-fabricate to form flocs under the hydraulic perturbation of leaching water and thus can be easily retained by the sand layer. In fact, LCU can easily flocculate in water solution and form a number of flocs with fractal structure (Fig. 3B). According to DLVO theory, this was because the ATP colloidal tended to be destabilized (flocculation) under the netting and bridging effect of P. Actually, a P macromolecule could bind a plenty of ATP colloidal particles at different sites of P probably through hydrogen bonds. Furthermore, these P macromolecules tended to crosslink each other making these ATP colloidal particles crosslink each other at the same time and form a number of flocs. The spatial scale and the morphology of the LCU floc are greatly affected by pH. As shown in Fig. 3B and 3C, with increasing pH, the average spatial scale of LCU flocs decreases owing to the increase of the zeta potential (absolute value). From Fig. 3A and the insets, networks are formed through the connection with each other among ATP, U and P. Moreover, the quality of networks is improved with the increase of pH due to the increase of the ATP dispersion in the flocs. Interestingly, the networks display an obviously different appearance at pH 12, as a plenty of separated long fibers appeared instead of ATP rods (Fig. 4C–E).

To explore the formation process of LCU networks and obtain the roles of the components (ATP, U and P), energy dispersive X-ray spectroscopy (EDX) and TEM analysis of the LCU flocs at pH 7.0 and 12 were investigated. As shown in Fig. 4A, three characteristic micro regions (MR) were chosen in the networks of LCU flocs at pH 7.0. The result demonstrated that, in MR (a), the feature elements of ATP (Al, Si and Mg) could not be determined except C, H, O and N, indicating that there was mainly U and P consisted in MR (a) to form penetrating networks (Fig. 4A(a)). MR (c) contained mainly ATP rods with a few organics on the surface, because the amounts of Al, Si and Mg were significantly higher than those of organic elements (Fig. 4A(c)). MR (b) was the transition state between (a) and (c), containing a lot of organics covering on the surface of ATP rods (Fig. 4A(b)).

At pH 12, a region containing aggregates appearing like ATP was found (Fig. 4B), from which a great number of fibrous crystals (length > 2 μm, diameter about 200 nm) grew in a radial pattern to form a pine needle-like crystal cluster. Organic elements (C, H, O and N) were enriched at the end of the crystals in MR (d), while the typical elements of ATP (Mg, Si and Al) were not detected (Fig. 4B(d)), which was verified by the inset TEM image in Fig. 4B(d). Specifically, due to the rather low content (2‰) of P within LCU, the detected organic component in the crystals was mainly urea. In the root MR (e) of the crystals (Fig. 4B(e)), Mg and Si were detected besides the organic elements, indicating that there were probably one or more ATP rods included in the urea fibers, which was in accordance with the inset TEM image in Fig. 4B(e). Furthermore, in the MR (f) (Fig. 4B(f)), more inorganic (Mg, Si and Al) and less organic elements were detected compared with the MR (e), illustrating that MR (f) was mainly undispersed ATP rods, which was verified by the inset TEM image in Fig. 4B(f). Therefore we conclude that the LCU networks at pH 12 are composed of urea-ATP crystal fibers which are initiated by ATP rods (crystal nucleus) and, thereafter, grow parallel to the longitudinal direction of the rods. Nevertheless, the LCU networks at pH 7.0 was fabricated by the connecting among these three components (ATP, U and P) other than long fibrous urea-ATP crystals as that at pH 12, because there is insufficient urea on the surface ATP rods to form such long urea-ATP crystals.

In order to further investigate the mechanism of the formation of the LCU networks, the interactions among the three components (ATP, U and P) were analyzed through Fourier transform infrared spectroscopy (FTIR). The band variations of P (-CONH₂), ATP (coordinated water, adsorption water, -OH and Si-O-Si) and U (NH₂, N-H) in the ATP-P, ATP-U, P-U and ATP-U-P systems were investigated as shown in Fig. 5. The detailed FTIR analysis (Supplementary discussion 1) suggested the formation of hydrogen bonds in these systems¹⁵. According to Lambert-Beer's Law ($A = \lg(1/T) = KLC$, where A is absorbance, T% is the transmission ratio, K is the absorption coefficient, and L and C are the thickness and concentration of the sample), with the same sample thickness, the weaker vibration peak, the lower concentration. With increasing pH, the amounts of adsorption water (H₂O), coordinated water (-OH₂) and hydroxy (-OH) of ATP as well as -NH₂ and -CO of P decrease, so do those of -NH₂, OCN and NCO of U, presenting the increase of hydrogen bonds formed in the ATP-P-U system with increasing pH. This was also proved by the SSNMR analysis (Supplementary Fig. 4). In addition, X-ray diffraction (XRD) and thermal analysis also confirm the formation of hydrogen bonds in the ternary LCU system (Supplementary Fig. 5 and Fig. 6).

Interactions among chemical groups of a multi-system in aqueous solution closely dependent on pH¹⁶. Specifically, hydrogen bonds play an important role in the interactions among molecules. For instance, hydrogen bonds are significant for super molecular self-fabrication¹⁷. Based on the preceding analysis, within an aqueous environment, the hydrogen bonds are probably the driving force of

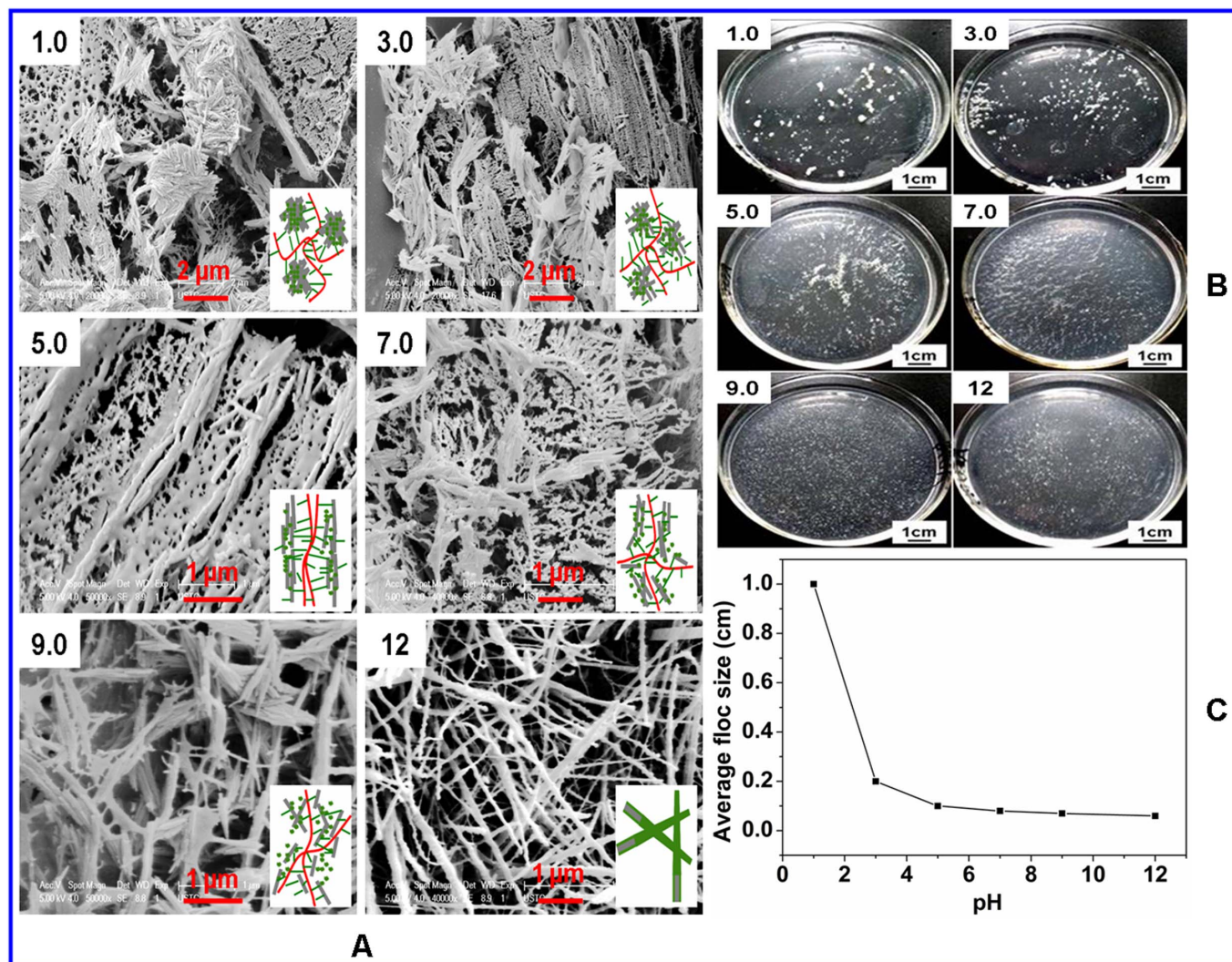


Figure 3 | Morphology of LCU flocs under different pH conditions. (A), SEM images of LCU (1 g/L) flocs under different pH conditions. Insets were the schemes of the corresponding structures (gray, red and green imply ATP rod, molecular assemblies of P and molecular assemblies of U respectively). (B), Digital photographs of LCU flocs in aqueous solutions at different pH values. (C), Average spatial scale (image method) of LCU flocs under different pH conditions.

the connection among these three components (ATP, U and P) or the formation of fibrous U-ATP crystals, which further self-fabricate (actually flocculate) to form 3D networks flocs. Moreover, the amount of the hydrogen bonds increases with the increasing pH, leading to different microstructures of the networks flocs, shown in Fig. 3A. According to DLVO theory¹⁸, the colloidal particles (ATP rods or ATP-U crystals) are destabilized by P to form flocs with fractal structure (networks), which enlarges the spatial scale of urea-N and thus achieve optimal control of N migration performance through the filtering effect of soil layer.

The average size of LCU flocs formed in aqueous solution at pH 7.0 was approximately 30 μm (Fig. 3C). In reality, soil is a special type of porous medium including three kinds of pores (non-active pores (feature diameter $< 2 \mu\text{m}$), capillary pores ($2 \mu\text{m} < \text{feature diameter} < 20 \mu\text{m}$) and aeration pores (feature diameter $> 20 \mu\text{m}$)). Therefore, with the flow of rainwater, these LCU flocs can neither pass through the non-active pores nor the capillary pores in soil. However, they can partly pass through the aeration pores. In the plough layer (20–50 cm deep), these three kinds of flexural and discontinuous pores interlace with each other. As a result, it is difficult for the aeration pores to penetrate directly or for a long distance into the plough layer. Thus, although the flocs, which are smaller

than the feature diameter of aeration pores, they will eventually be stopped at another place in the plough layer. Thus the migration of nitrogen with high spatial scales can be effectively controlled, which has been verified via the leaching, volatilization and runoff behaviors comparison between LCF (N^{15} -LCU or LCN) and traditional fertilizer (U or NH_4Cl). Under simulated conditions, about 50% leaching (Fig. 6A), 36% volatilization losses (accumulating for 20 days) (Fig. 6B) and 45% surface runoff (Fig. 6C) of N can be reduced by this loss control technology, which can also effectively control the leaching of NH_4^+ and HPO_4^- and NH_3 volatilization in soil with different spatial scales (Supplementary Fig. 7–10). These results display an obvious loss control capacity of LCF.

Discussion

We further tested if adsorption caused the loss control function of LCU, believed to be related to weak interactions among U, ATP and P. XRD analysis (Supplementary Fig. 5) showed that although ATP consists of multiple nano-pores, only a few urea molecules were able to access these, as the pores were too small ($3.7 \times 6.3 \text{ nm}$). Nevertheless these pores were relatively accessible for NH_3 , whose molecular scale is smaller than that of urea. This was indicated in an

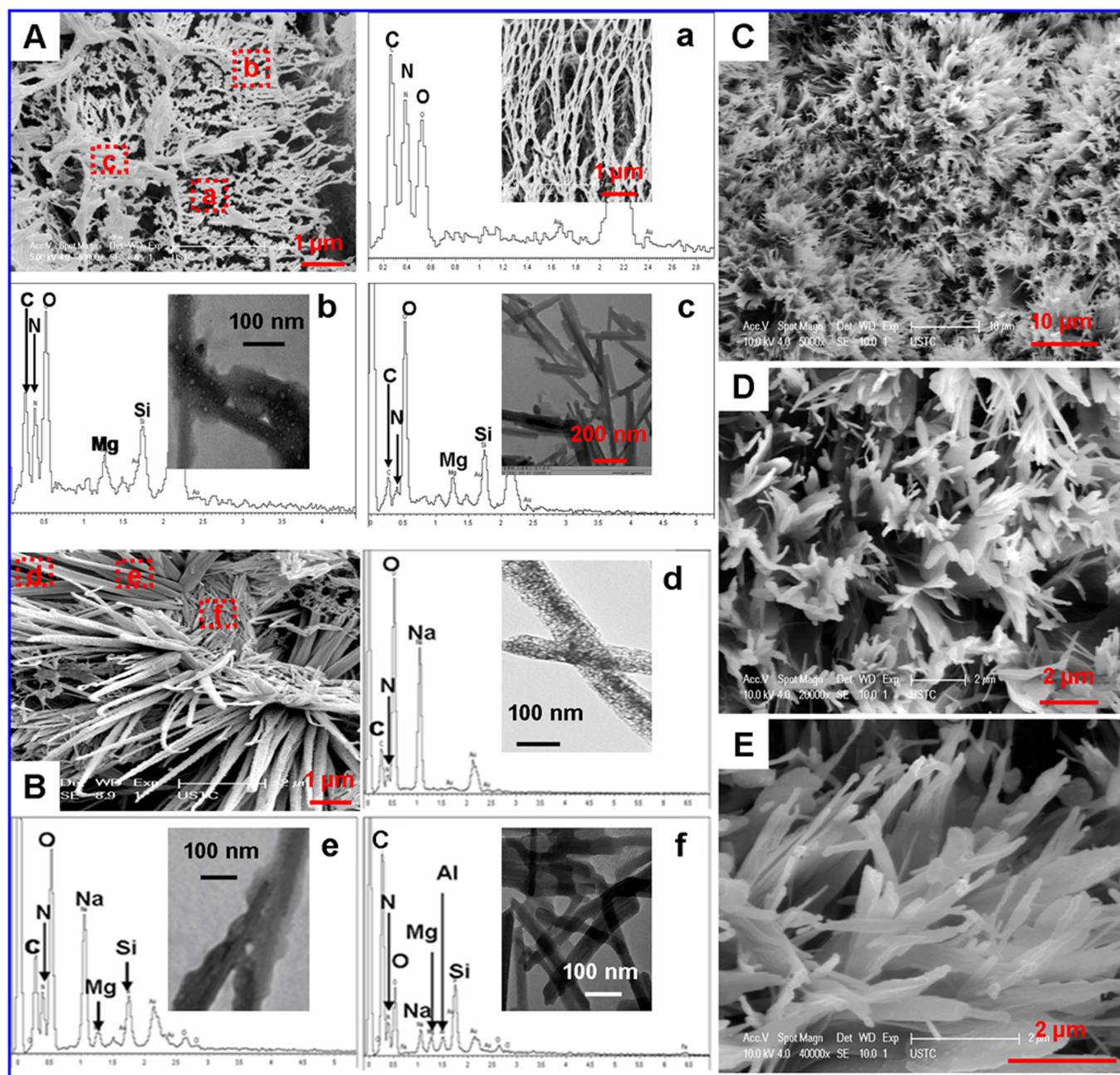


Figure 4 | Morphology and EDX analysis of LCU flocs. (A–E), SEM images of LCU flocs under pH conditions of 7.0 (A) and 12 (B–E) with different magnification. (a–c) and (b–f), Main elements (EDX analysis) contained in the corresponding micro regions in (A) and (B) respectively. Insets are SEM (a) or TEM (b–f) images for the corresponding micro regions.

adsorption experiment. In urea aqueous solution (0.9 g/L) at room temperature, the maximum adsorption amount of urea on ATP (0.1 g/L) was approximately only 20 mg/g. Generally, chemical adsorption always accompanied chemical change, while few obvious chemical change in LCU was found (Fig. 5), illustrating that there was no obvious chemical adsorption. These results suggest that adsorption is not the main mechanism of LCU. Otherwise, the 3D micro/nano networks, self organized by ATP and organic ligands (U and P) through hydrogen bonds and molecular force, were probably the main cause for migration prevention of urea in soil and reduction of NH_3 volatilization.

In aspects of application, the agricultural effects of LCF consisting of 4%–5% (mass ratio) LCA, were also considered and investigated (Supplementary Fig. 11). Large-scale field tests demonstrated that, compared with traditional fertilizer, the yield of crops using LCF

was kept equal with 20% lower nutrition, while the yield improved more than 10% with equal nutrition. Furthermore, after harvest, the residual amount of N in the soil (20 cm deep) using LCF was greater (more than 10%) than that of traditional fertilizer (Supplementary Fig. 12), which could be absorbed by crops in the next season. Importantly, LCU and its components could significantly improve the cation exchange capacity (CEC) of soil to varying degrees (Supplementary Fig. 13), implying that the application of LCU also facilitated the enhancement of water and nutrition retention ability of soil¹⁹.

In summary, to control nitrogen migration, herein we have developed a new fertilizer named LCU through the addition of ATP and P to urea. The LCU can self fabricate to form 3D micro-nano networks flocs within aqueous environment through the connection among these three components (ATP, U and P) or the construction of fibrous U-ATP crystals, which is probably driven

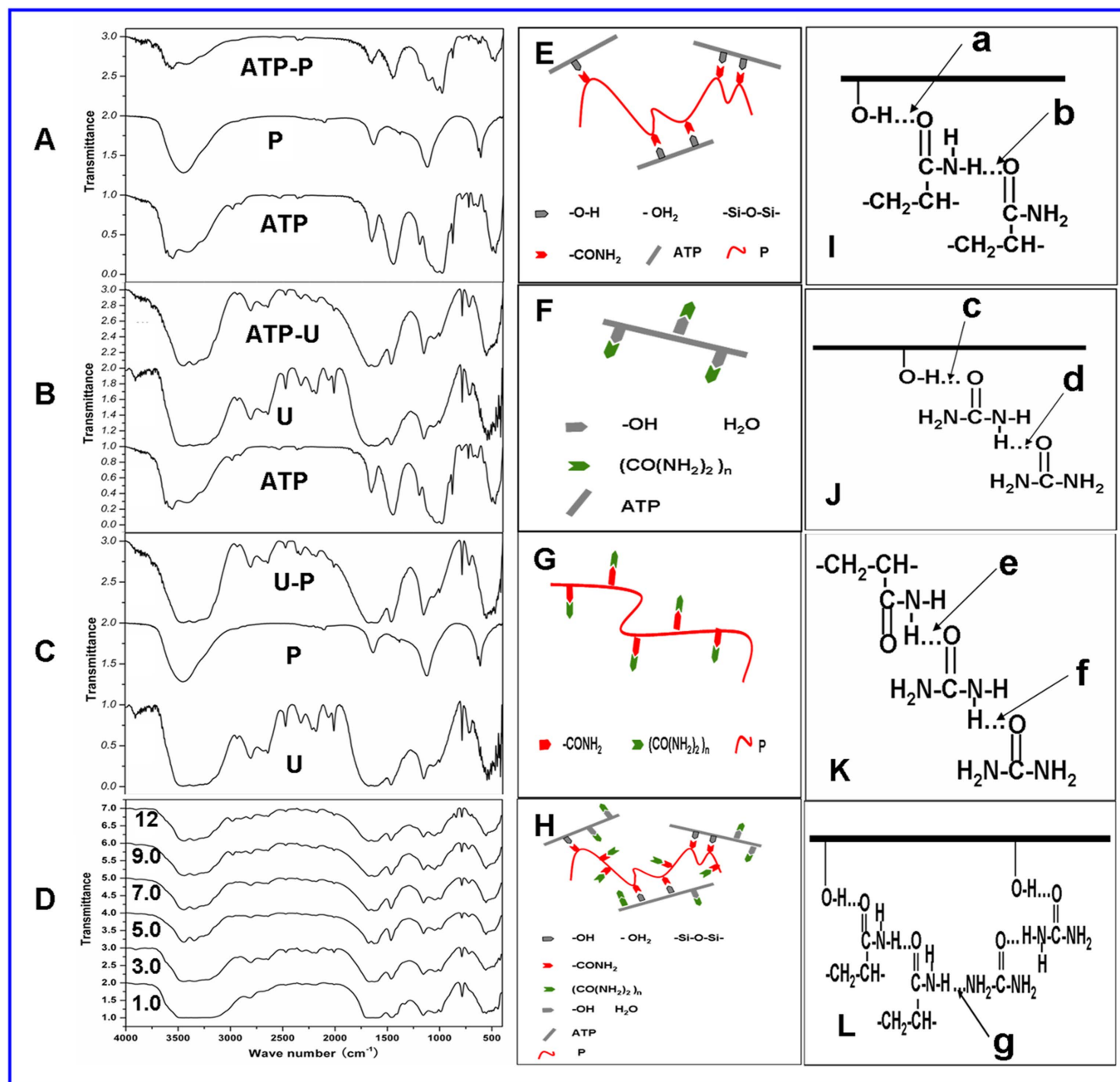


Figure 5 | FTIR analysis of ATP-P-U system (actually LCU). (A–C), FTIR spectra of ATP-P, ATP-U and U-P systems prepared at pH 7.0. (D), FTIR spectra of ATP-P-U system prepared under different pH conditions. (E–L), Schemes of hydrogen bonds in ATP-P (E, I), ATP-U (F, J), U-P (G, K) and ATP-P-U (H, L) systems, respectively. (a–g), Hydrogen bonds.

by the hydrogen bonds formed in the LCU system. The resulting LCU flocs possess higher spatial scales than the soil pores, so that the migration of nitrogen in soil can be effectively controlled, which has been verified by the leaching, volatilization and runoff investigations. In other words, LCU is able to effectively reduce the risk of N transfer into the environment while providing sufficient nutrients for crops. In all, this article provides a promising approach for controlling nitrogen migration and loss through micro-nano networks, which might be potentially used to control the migration of other micro pollutants in environment medium.

Methods

The samples were prepared as follows. Raw attapulgite (purity of 95%, 200 mesh size) was irradiated by high-energy electron beam (10 MeV, 40 kGy) to improve its dispersion and then its suspension (10 g/L) was treated by O_3 (200 g/h) with an ozone

generator (WH-G-2-250, Nanjing WoHuan Co., China) for 30 min to remove the organic purities and increase the $-OH$ number on the surface of attapulgite. The resulting suspension was dried ($80^\circ C$) and ground to powders (200 mesh size) after hydrothermal treatment ($180^\circ C$) for 2 hours to further improve the dispersion of attapulgite. Afterwards, the resulting ATP was mixed with P (nonionic, 100 mesh size, molecular weight of 5–10 million) with the mass ratio of 50:1 to obtain LCA, which was thereafter added (10%, weight) to urea (or NH_4Cl) to obtain LCU (or LCN). The samples (ATP-U, U-P, ATP-P and LCU) (Supplementary table 1) for characterizations (SEM (Sirion200, FEI Co., USA), TEM with energy dispersive X-ray spectroscopy (EDX) (JEOL – 2010, JE Co., Japan), FTIR (Bruker Co., Germany), TGA (DTG-60H, Shimadzu Co.), Solid state nuclear magnetic resonance (SSNMR) (AVANCE III 400, Bruker Co., Switzerland), Zeta potential (Zetasizer 3000, Malvern UK), X-ray imaging on synchrotron radiation (SSRF) and XRD (TTR-III, Rigaku Co., Japan)) were prepared through the following approach. The hybrids (ATP-U (50:459), U-P (50:459), ATP-P (50:1) or ATP-P-U (50:1:459, W/W)) were soaked in aqueous solution (3 g/L) respectively, and dried ($60^\circ C$) to constant weight after being stirred for 2 min.

To obtain the loss control property through leaching, the migration performance of loss control NH_4Cl (LCN) (1 g) or NH_4Cl (0.9 g) from the top of perlite column

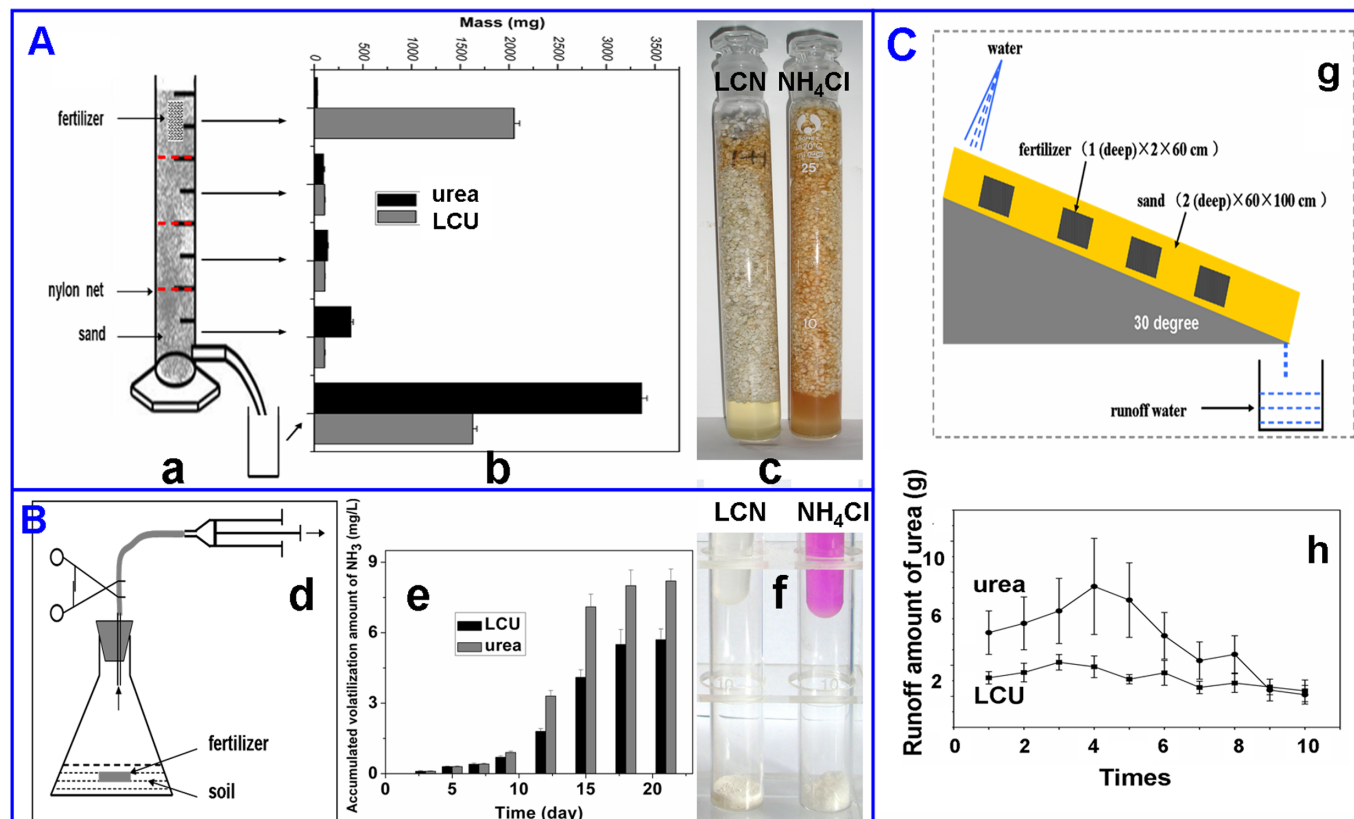


Figure 6 | Loss control performance of LCF through leaching (A), volatilization (B) and runoff (C). (a), Sand column. (b), Residue amounts of LCU in each sand layer after leaching compared with urea. (c), Migration performance of loss control NH₄Cl (LCN) and NH₄Cl in perlite columns. (d), Volatilization determination system. (e), Accumulated NH₃ volatilization amounts of LCU and urea with time. (f), NH₃ volatilization capacity difference between LCN and NH₄Cl. (g), Runoff determination system. (h), Urea loss amounts of LCU and urea with runoff times.

(20 cm high) immersed in Na's reagent was investigated. NH₄⁺ distribution in the column could be observed directly after 20 min through Na's reaction (NH₄⁺ could react with Na's reagent to generate yellow-colored substance, and the color depth reflects the concentration of NH₄⁺). Besides, the leaching performance of LCU in sand column was determined through the following procedure. Sample (urea (0.9 g) or LCU (1 g), N¹⁵ labeled at the abundance of 30%) was buried (cylinder shape, diameter of 1.0 cm and depth of 2 cm) within the top layer of a sand column (25 cm high) which was saturated with water and separated to 4 layers by nylon nets. 100 mL water was sprayed (3 mL/min) over the top layer to get 100 mL leachate. Afterwards, the sand within each layer was washed with distilled water and then centrifuged to obtain the supernate. Urea contents and the N¹⁵ abundance were detected through armour amino benzaldehyde method and Isotope mass spectrometer (MAT 271, Finnigan Co. USA) respectively.

To evaluate the volatilization property, NH₃ volatilization capacity of LCN (1 g) or NH₄Cl (0.9 g) was investigated directly in a sealed tube (25 mL) after 20 min at 30°C through reaction with phenolphthalein reagent (1.5 mL) in 2 ml tube suspended at top of the sealed tube. Moreover, accumulated NH₃ volatilization amounts of LCU (3 g) or urea (2.7 g) buried (1 cm deep, cuboid-shape of 1 × 2 × 3 cm) in soil (200 g, humidity of 30%) in a sealed flask with time were investigated at 30°C. 10 mL gas in the sealed flask was taken out and put into Na's solution for each time, afterwards 10 mL fresh air was put into the sealed flask immediately. The NH₄⁺ concentration in the solution was determined through Na's colorimetric method using UV/VIS spectrometry (TU-1901, Beijing Pu Xi Tong Yong Instruments Corp.).

Runoff loss performance was investigated through the following procedure. Sample (60 g LCU or 54 g urea) was buried paralleled (every 20 cm along the slope direction, 1 cm deep, cuboid shape of 1 × 2 × 60 cm) in sand (humidity of 30%) on PVC sloping panel (30 degree, 1 m × 1 m, two near edges were enclosed) at 30°C. 3 L water was sprayed each time over the top layer and the runoff water was collected and detected through armour amino benzaldehyde method.

- Gregory, F. M. *et al.* Eutrophication: Nitrate flux in the Mississippi River. *Nature* **414**, 166–167 (2001).
- Reay, D. S. *et al.* Global agriculture and nitrous oxide emissions. *Nature Clim. Change* **2**, 410–416 (2012).
- Guo, J. H. *et al.* Significant acidification in major chinese croplands. *Science* **327**, 1008–1010 (2010).

- Erismann, J. W. *et al.* How a century of ammonia synthesis changed the world. *Nature Geosci.* **1**, 636–639 (2008).
- Metz, B. *et al.* Intergovernmental Panel on Climate Change (IPCC), 2007. Climate Change 2007: Mitigation. *Contribution of Working Group III to the Fourth Assessment Report of the Intergovernmental Panel on Climate Change* (Cambridge Univ. Press, Cambridge and New York, 2007).
- Juo, A. S. R. *et al.* Acidification of a kaolinitic alfisol under continuous cropping with nitrogen fertilization in West Africa. *Plant Soil* **171**, 245–253 (1995).
- Matsuyama, N. *et al.* Acidification and soil productivity of allophanic andosols affected by heavy application of fertilizers. *Soil Sci. Plant Nutr.* **51**, 117–123 (2005).
- Richter, Andreas *et al.* Increase in tropospheric nitrogen dioxide over China observed from space. *Nature* **437**, 129–132 (2005).
- Li, H. P. *et al.* The non-point output of different landuse types in Zhexi hydraulic region of Taihu basin. *Acta Geog. Sinica* **59**, 401–408 (2004).
- Gullett, L. L. *et al.* Sulfur coating of urea treated with attapulgite clay. *Fert. Res.* **28**, 123–128 (1991).
- Williams, K. A. & Nelson, P. V. Phosphate and potassium retention and release during chrysanthemum production from precharged materials: II. calcined clays and brick chips. *JAM Soc. Hortic. Sci.* **125**, 757–764 (2000).
- Li, A. *et al.* Preparation and slow-Release property of a poly(acrylic acid)/attapulgite/sodium humate superabsorbent composite. *J. Appl. Polym. Sci.* **103**, 37–45 (2007).
- Ni, B. L. *et al.* Environmentally friendly slow-Release nitrogen fertilizer. *J. Agric. Food Chem.* **59**, 10169–10175 (2011).
- Galán, E. Properties and applications of palygorskite–sepiolite clays. *Clay Miner.* **31**, 443–453 (1996).
- Grdadolnik, J. & Maréchal, Y. Urea and urea-water solutions-an infrared study. *J. Mol. Struct.* **615**, 177–189 (2002).
- Wang, Q. *et al.* Preparation and characterization of a novel pH-sensitive chitosan-poly (acrylic acid)/attapulgite/sodium alginate composite hydrogel bead for controlled release of diclofenac sodium. *Carbohydr. Polym.* **78**, 731–737 (2009).
- Jeffrey, G. A. An introduction of hydrogen bonding (Oxford Univ. Press, New York, 1997).
- Yang, Z. *et al.* Evaluation of the flocculation performance of carboxymethyl chitosan-graft-polyacrylamide, a novel amphoteric chemically bonded composite flocculant. *Water Res.* **46**, 107–114 (2012).



19. Hendershot, W. H. & Duquette, M. A simple barium chloride method for determining cation exchange capacity and exchangeable cations. *Soil Sci. Soc. Am. J.* **50**, 605–608 (1986).

Acknowledgments

The authors acknowledge financial support from the National Natural Science Foundation of China, Anhui province, Ningxia province, Chinese Academy of Sciences and The Chinese Ministry of science and technology: No. 10975154, 1206c0805014, 08010302117, 10975145, KSZD-EW-Z-022-05, KSCX2-YW-N-080. The authors also acknowledge the X-ray imaging (BL13W) and the scanning and transmission X-ray microscopy (BL08U) work stations on Shanghai Synchrotron Radiation Facility (SSRF) for the microstructure observation, and the hard X-ray microscopy work station on National Synchrotron Radiation Laboratory (NSRL) of China for the help of the data analysis. Additionally, we thank S. Yu for his kindly revision of this article, L.F. Wu for her contribution to the application of LCF, N. Wang and G.L. Zhang for their constructive suggestions.

Author contributions

D.Q.C. and Z.Y.W. carried out most of the experiments and analyzed the data at the supervision of Z.L.Y.; J.J. and H.Y.F. contributed to the sample preparation and N loss performance determination; Y.J.W. performed the field experiment; I.G.B. and P.K.C. advised and revised the manuscript; all authors discussed the results and commented on the manuscript.

Additional information

Supplementary information accompanies this paper at <http://www.nature.com/scientificreports>

Competing financial interests: The authors declare no competing financial interests.

How to cite this article: Cai, D.Q. *et al.* Controlling nitrogen migration through micro-nano networks. *Sci. Rep.* **4**, 3665; DOI:10.1038/srep03665 (2014).



This work is licensed under a Creative Commons Attribution-NonCommercial-ShareAlike 3.0 Unported license. To view a copy of this license, visit <http://creativecommons.org/licenses/by-nc-sa/3.0>